PCCP

Reactions of the •NO3 radical with nuclear extraction ligands in alkane solution

Journal:	*Physical Chemistry Chemical Physics*
Manuscript ID	CP-ART-02-2024-000751.R3
Article Type:	Paper
Date Submitted by the Author:	24-Jul-2024
Complete List of Authors:	Dang, Anh; California State University at Long Beach, Chemistry and Biochemistry Rogalski, Maya ; California State University Long Beach, Department of Chemistry and Biochemistry Peterman, Dean; Idaho National Laboratory, 1765 N. Yellowstone Hwy Mincher, Bruce; Idaho National Laboratory Mezyk, Stephen; California State University at Long Beach, Chemistry and Biochemistry

Reactions of the $^{\bullet}NO_3$ radical with nuclear extraction ligands in alkane solution

Anh N. Dang[a], Maya H. Rogalski[a], Dean R. Peterman[b], Bruce J. Mincher[b], Stephen P. Mezyk*[a]

a California State University at Long Beach, Department of Chemistry and Biochemistry, 1250 N. Bellflower Blvd., Long Beach, CA, 90840, USA, E-mail: Stephen.Mezyk@csulb.edu

b Idaho National Laboratory, Center for Radiation Chemistry Research, PO Box 1625, Idaho Falls, ID, 83415, USA

ORCID Numbers:

Anh N. Dang	0009-0007-1090-5945
Maya H. Rogalski	0009-0009-3435-2999
Dean R. Peterman	0000-0003-4374-6948
Bruce J. Mincher	0000-0003-3108-2590
Stephen P. Mezyk	0000-0001-7838-1999

The reactivity of the nitrate radical ($NO_3^{\bullet}$) with organophosphorous and amidic actinide and lanthanide complexing agents of interest to nuclear solvent extraction applications was measured, resulting in the first-ever reported bimolecular rate constants for this radicals' reactions in dodecane solution. The order of reactivity for neutral organophosporous compounds showed faster rate constants with increasing electron density on the phosphoryl carbon, indicating an increasing facility for electron abstraction reactions occurring in addition to H-atom abstraction from the ligand alkane chains. The only acidic organophosphorous compound investigated, HEH[EHP], showed low reactivity with $NO_3^{\bullet}$ radical, attributed to its dimerization in this non-polar solvent. Amide ligand reaction rates were faster than for organophosphorous molecules, suggesting more facile H-atom abstraction from carbonyl activated methylene and amyl groups. While all rate constants were slower than the diffusion-limited rate they were still rapid enough to result in significant oxidation of solvent extraction ligands in dodecane solution.

Introduction:

Uranium and plutonium have been successfully recycled from dissolved nuclear fuel solutions using tributyl phosphate (TBP) for almost 80 years, beginning in the Manhattan Project of World War II.[1] This neutral organophosphorous ligand solvates uranium and plutonium ions in aqueous nitric acid as neutral nitrate complexes, which allows their partitioning to an organic phase consisting of an alkane diluent:

$$UO_2^{2+} + 2TBP + 2NO_3^- \rightleftharpoons [UO_2(NO_3)_2(TBP)_2] \quad (1)$$

$$Pu^{4+} + 2TBP + 4NO_3^- \rightleftharpoons [Pu(NO_3)_4(TBP)_2] \quad (2)$$

However, TBP is inefficient for the extraction of trivalent actinides and lanthanides. This has been exploited to allow for the separation of uranium and plutonium from each other by redox manipulation of the plutonium valence state to Pu^{3+}. Tributyl phosphate chemistry has been extensively reviewed by Schulz and Navratil in a multi-volume series.[2]

To develop a group actinide/lanthanide complexing agent that co-extracts trivalent metals, neutral organophosphorous compounds with more basic phosphoryl oxygen atoms are needed. Increased basicity is achieved by replacing the ether linkages of the phosphate with alkanes, to produce phosphonates and phosphine oxides having increased electronegativity on the phosphoryl O-atom.[3] As an alternative to organophosphorous compounds, neutral, amidic O-donor ligands such as monoamides and diamides are also employed as group extractants for the actinides and lanthanides,[4,5] with the added advantage that they can be incinerated for waste treatment purposes at the end of their useful lifetime. This is the so-called CHON principal in which the ligand is composed of only C, H, O and N atoms.[6]

Nuclear fuel dissolutions are highly radioactive due to decay of the dissolved actinides, fission products and activation product components of used fuel. Regardless of the solvent

extraction approach chosen, the organic ligands employed in contact with acidic, nuclear fuel dissolutions must be stable in the presence of the reactive species produced by the multi-component radiolysis of both water and acid. For example, Elias *et al*. showed that the gamma-irradiation of the aromatic compound anisole in aqueous nitric acid produced the same products as thermal acid hydrolysis, only in greater yields.[7] Thus, the degradation of ligands in irradiated nitric acid is to be expected, along with its attendant, often detrimental, effects on metal ion separation efficiencies. One of the most important reactive species in irradiated nitric acid solution is the nitrate radical ($NO_3^\bullet$),[8] produced by both direct (⇝) and indirect radiolysis of both nitrate and nitric acid:[9–13]

$$HNO_3 \rightsquigarrow HNO_3^+ + e^- \rightarrow H^+ + NO_3^\bullet + e^- \quad (3)$$

$$NO_3^- \rightsquigarrow NO_3^\bullet + e^- \quad (4)$$

$$H_2O \rightsquigarrow H_2O^+, e^-, H_2O^* \rightarrow OH^\bullet, H^\bullet, e^-, H_2O_2, H_2, H^+ \quad (5)[14]$$

$$HNO_3 + H^\bullet \rightarrow NO_3^\bullet + H_2 \quad (6)$$

$$HNO_3 + OH^\bullet \rightarrow NO_3^\bullet + H_2O \quad (7)$$

$$HNO_3 + H_2O^+ \rightarrow NO_3^\bullet + H_2O \quad (8)[15]$$

The $NO_3^\bullet$ radical is a reactive, oxidizing species that has received much attention due to its role in atmospheric chemistry,[16,17] where it is produced by the reaction of atmospheric NO_2 with O_3. Atmospheric NO_2 is largely present from the burning of biomass and fossil fuels, production by lightning, and due to soil microbial metabolism.[18] The $NO_3^\bullet$ radical is photolyzed back to NO_2 in daylight but is an important intermediate in the nighttime atmosphere and is thus ubiquitous in the natural environment. The $NO_3^\bullet$ radical reacts with organic compounds to produce nitro-derivatives in both the gas and aqueous phases. As such, a large body of its gas phase and aqueous condensed-

phase kinetic data have been acquired. However, these data have only limited use in understanding reactions in the highly acidic solutions of nuclear fuel reprocessing.

Of more direct interest are kinetic studies for the $NO_3^{\bullet}$ radical in irradiated nitric acid. For the higher concentrations of nitric acid used in most nuclear applications, it can be seen from Equation 7 that although radiolytically produced $OH^{\bullet}$ radical is produced in Equation 5, it is highly oxidizing and essentially quantitatively converted to $NO_3^{\bullet}$, which therefore becomes the most important oxidizing reactive species in this system. In previous work we found that $NO_3^{\bullet}$ is relatively long-lived in water ($\tau_{1/2} \sim 50$ μs) and we measured its reactivity in pulse-irradiated 5.0–6.0 M HNO_3 solutions.[19] Horne *et al*., reported $NO_3^{\bullet}$ reaction rate constants for a series of hydrophilic diglycolamides in irradiated aqueous neutral nitrate solution, which was performed to isolate radiolytic effects from acid hydrolysis.[20] The latter study reported dose constants (kGy^{-1})[21] for ligand degradation and identified nitro-derivatives among the degradation products for steady-state, gamma-irradiated solutions.

Under nuclear waste extraction process conditions, the organic phase itself will also contain nitric acid following contact with the aqueous phase and the acid may be present at fairly high concentrations, both as a complex with the neutral ligand and entrained in extracted water. For example, Ferraro *et al*., identified TBP/HNO_3 solvates in octane[22] and Horne *et al*., identified monoamide/HNO_3 solvates in dodecane by IR analysis.[23] Similarly, HNO_3 complexes with the neutral organophosphorous extractant octylphenyl-(N,N-) diidobutylcarbamoylmethyl phosphine oxide (CMPO) have been identified by mass spectrometry,[24,25] and are anticipated for other neutral, basic ligands as well.[26,27] Bell *et al*., measured concentrations of extracted nitric acid in a TODGA/odorless kerosene solution that equaled the ligand concentration for contact with 3 M HNO_3 solutions and exceeded the ligand concentration for contacts with higher acidity.[28]

The radiolysis of nitric acid in the organic phase will also result in the formation and accumulation of $NO_3^{\bullet}$ radicals, which can then react with ligand and diluent molecules to generate corresponding nitro-derivatives. These $NO_3^{\bullet}$ reactions have not been previously investigated in liquid alkanes, due to the difficulty in finding a source of nitrate soluble in non-polar solution. It is known that $NO_3^{\bullet}$ reactions are faster in less polar solvents, due to increased mobility in solutions of low dielectric strength.[29] We have previously reported rate constants for this radical with organic solutes that are faster than aqueous for *t*-butanol, using the electron pulse radiolysis of 1.25 M tetrabutyl-ammonium nitrate and NH_4NO_3 solutions.[19] In acetonitrile, the higher solubility of the anion of ceric ammonium nitrate, $Ce^{IV}(NO_3)_6^{2-}$ allows for the use of laser photolysis to generate $NO_3^{\bullet}$ radical directly, and extensive kinetic investigations of $NO_3^{\bullet}$ with organophosphorous ligands have been reported in that medium.[19,30] However, there are no reports concerning $NO_3^{\bullet}$ radical reactions in the alkane solutions of importance to nuclear fuel cycle solvent extraction separations. Thus, in this work we developed a method to generate, detect, and measure the reaction kinetics of alkane-phase $NO_3^{\bullet}$ radical to better understand its effect on nuclear solvent extraction processes. The structures of the organophosphorous ligands used here are given in Figure 1, those of the amides are shown in Figure 2.

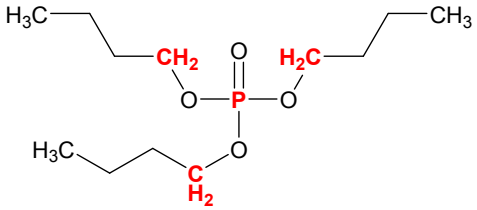

tributylphosphate (TBP)

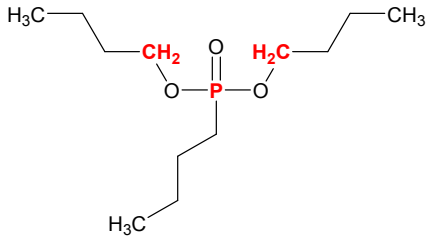

dibutylbutylphosphonate (DBBP)

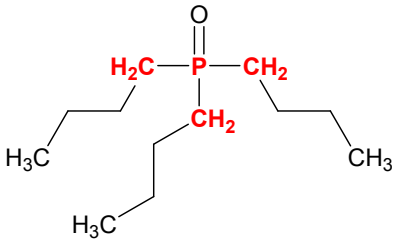

tri-*n*-butylphosphine oxide (TBPO)

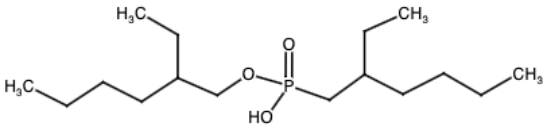

2-ethylhexylphosphonic acid mono-2-ethylhexyl ester (HEH[EHP])

Fig. 1 Structures of the neutral organophosphorous oxygen donors and the acidic HEH[EHP] ligands investigated in this study. Dominant reaction sites marked in red.

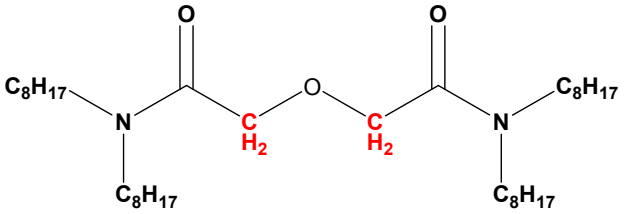

N,N,N',N'-tetra-*n*-octyl-3-oxapentanediamide (TODGA)

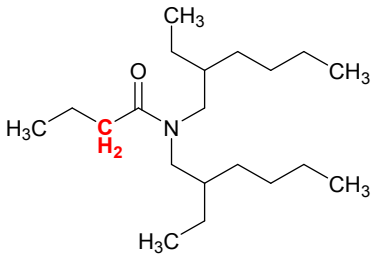

di-2-ethylhexylbutyramide (DEHBA)

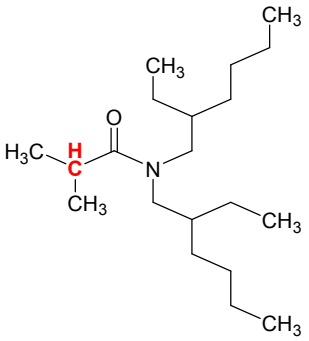

di-2-ethylhexylisobutyramide (DEH*i*BA)

Fig. 2 Structures of the amidic neutral oxygen donor ligands investigated in this study. Dominant reaction sites marked in red.

Methods

Laser photolysis

The reaction kinetics of $NO_3^\bullet$ were measured using a pulsed exciplex laser (Lambda Physik XeCl* at 308 nm) at the Radiation Research Laboratory at the University of Notre Dame. The laser had a pulse energy of ~28 mJ, a pulse width of ~20 ns and was operated at a frequency of 1 Hz. The $NO_3^\bullet$ radical has a characteristic strong absorbance at 620-640 nm[31] with little variation in its absorption spectra for different solvents,[19] making its detection straightforward. Experiments were conducted in 6-mm quartz flow cuvettes at room temperature (22 ± 2 °C). The laser flash photolysis of ceric ammonium nitrate $(NH_4)_2Ce^{IV}(NO_3)_6$ directly generated $NO_3^\bullet$ in the organic phase: [30,32,33]

$$[Ce^{IV}(NO_3)_6]^{2-} + h\nu \rightarrow [Ce^{III}(NO_3)_5]^{2-} + NO_3^\bullet \quad (9)$$

Sample preparation

A stock solution of ceric ammonium nitrate in *n*-dodecane was prepared via solvent extraction. An aqueous phase was made by dissolving 4-8 mM ceric ammonium nitrate in 6 M HNO_3. An organic phase composed of 48-60 mM TBP in *n*-dodecane was pre-washed thrice with 0.25 M Na_2CO_3 and once with 0.1 M HNO_3 at a 1:2 aqueous to organic ratio to remove any phosphoric acid impurities. Equal volumes of the aqueous and organic phases were then vigorously mixed for 5 minutes in a separatory funnel. After phase separation, the organic phase containing the extracted ceric ammonium nitrate was used to dilute the ligand in dodecane solutions to the desired ligand concentrations. Organic phase CAN concentrations were confirmed by ICP-MS measurements. Typically, 25 mL of each ligand solution was made, and gravity fed through the 6 x 10 mm flow cell at a rate sufficient to ensure that each kinetic measurement was performed on a fresh sample. Kinetic traces were the average of 4-16 individual pulses.

Materials

Unless otherwise indicated the solvent extraction ligands were obtained from on-hand stock at the Idaho National Laboratory and diluted directly in *n*-dodecane (Thermo Scientific, 99%). The neutral phosphoryl donors were 2.5–10 mM dibutylbutylphosphonate (DBBP), 2.5–10 mM tri-*n*-butylphosphine oxide (TBPO) and 60–150 mM tributylphosphate (TBP, Sigma-Aldrich, $\leq$ 99%). The neutral amidic donors were 0.1–1.5 mM N,N,N',N'-tetra-*n*-octyl-3-oxapentanediamide (TODGA), 0.1–1.5 mM di-2-ethylhexylbutyramide (DEHBA), 2.5–10 mM di-2-ethylhexylisobutyramide (DEH*i*BA). Additionally, one acidic organophosphorus ligand was investigated, 2-ethylhexylphosphonic acid mono-2-ethylhexyl ester ((HEH[EHP]), Marshallton Research Laboratories, 98%), over the concentration range 0.2 –30 mM. Its structure is also given in Figure 1. The following additional reagents, used without further purification, were nitric acid (HNO_3, Sigma-Aldrich, 70 wt%), sodium carbonate (Na_2CO_3, BDH, ACS grade) and ceric ammonium nitrate ($(NH_4)_2Ce^{IV}(NO_3)_6$, Sigma-Aldrich, 99.99%). Aqueous solutions were prepared using deionized water (MilliQ, 18.2 MΩ-cm).

Results and discussion

Because ceric ammonium nitrate is itself an oxidizing agent (+1.44 V vs SHE)[34] we first investigated the possibility that it would thermally react with the organic solutions. Solutions of 0.5–10 mM ceric ammonium nitrate (CAN) in 50 mM TBP/*n*-dodecane were mixed in a 1:1 volume ratio with 10 mM ligands in *n*-dodecane. The UV-visible spectra of these solutions showed < 10% change in CAN absorbance after 24 hours in the dark, indicating that its thermal reaction with the ligand would not be significant for the 1–2-hour timescales of the laser kinetic studies.

Typical kinetics for the reactivity of the $NO_3^\bullet$ radical, as measured at 640 nm, are shown in Figure 3a for the ligand DEH*i*BA. At higher ligand concentrations these pseudo-first-order decays became faster. These measured decays were fit to a single-exponential decay function:

$$Abs = Abs^o * e^{-k't} + B \quad (10)$$

where Abs is the measured absorbance at time t, Abs^o is the initial absorbance at time zero, B is a baseline adjustment parameter and k' is the pseudo-first-order rate constant (s^{-1}) for the $NO_3^\bullet$ reactivity.

Our solution preparation of mixing ceric ammonium nitrate/TBP with different volumes of stock ligand solutions resulted in slightly different concentrations of ceric ammonium nitrate/TBP for each ligand concentration measurement. As such, the overall fitted k' value was the sum reactivity of three separate reactions:

$$NO_3^\bullet + [Ce^{IV}(NO_3)_6]^{2-} \rightarrow \text{products} \quad (11)$$

$$NO_3^\bullet + TBP \rightarrow \text{products} \quad (12)$$

$$NO_3^\bullet + \text{ligand} \rightarrow \text{products} \quad (13)$$

with the overall pseudo-first-order rate constant at each ligand concentration being:

$$k' = k_{11}*[Ce^{IV}(NO_3)_6]^{2-}] + k_{12}*[TBP] + k_{13}*[Ligand] \quad (14)$$

To correct the fitted first-order k' to find only k_{13} for the reaction of $NO_3^\bullet$ with the ligands, the ceric ammonium nitrate concentration was varied from 8–32 mM at a constant TBP concentration of 50 mM in dodecane, giving $k_{11} = (2.18 \pm 0.13) \times 10^7$ $M^{-1}s^{-1}$. Similarly, by varying the TBP concentration from 60–150 mM at a constant ceric ammonium nitrate concentration a value of $k_{12} = (1.17 \pm 0.26) \times 10^7$ $M^{-1}s^{-1}$ was determined. These k_{11} and k_{12} rate constants were then used to correct all the other fitted k' values for the different ligand concentrations. The blank (0 mM ligand) trace shown in Figure 3a, corresponds to the fitted value of $k' = (4.13 \pm 0.06) \times 10^5$ s^{-1} in

Figure 3b. The values of k' at other ligand concentrations were corrected using k_{11} and k_{12} as shown in Equation 14, and by then plotting the corrected k' values as a function of ligand concentration, resulting in the second-order rate constant k_{13} = (7.98 ± 0.80) x 10^7 $M^{-1}s^{-1}$for DEH*i*BA, from the data shown in Figure 3. The second-order rate constants k for the reactions of NO_3• with all the species of this study are given in Table 1.

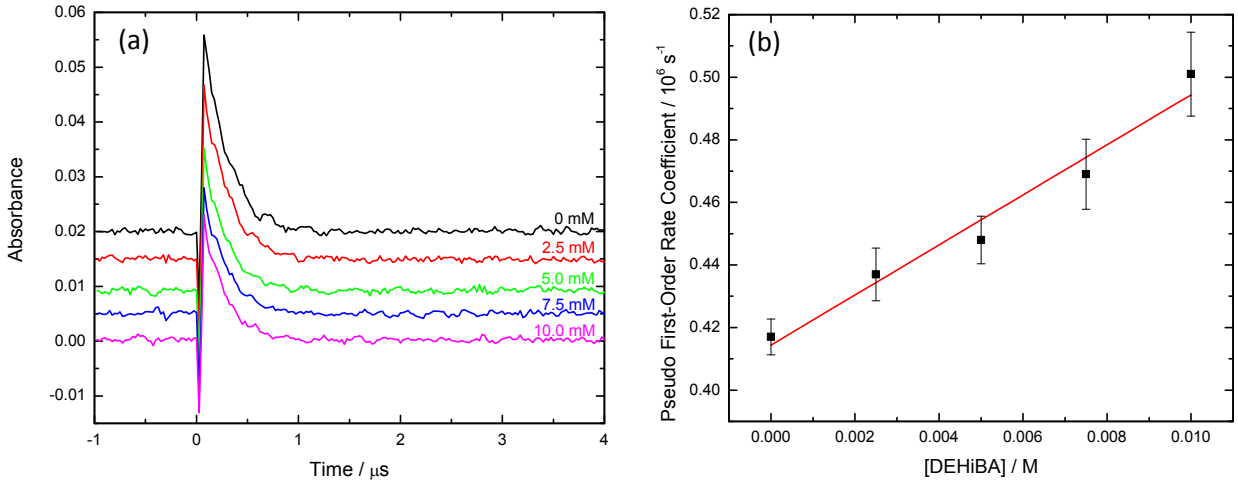

Fig 3. (a) Kinetic traces measured at 640 nm for NO_3• reaction with 0–10 mM DEH*i*BA, offset to aid clarity. (b) Linear fit of corrected pseudo first-order rate constant (k') as a function of DEH*i*BA concentration, corresponding to a second-order rate constant k_{13} = (7.98 ± 0.80) x 10^7 $M^{-1}s^{-1}$.

Table 1. Second-order rate constants (k) for the reaction of $NO_3^\bullet$ with the compounds investigated in this study.

Ligand	Rate Constant ($M^{-1}s^{-1}$)
ceric ammonium nitrate (CAN)	$(2.18 \pm 0.13) \times 10^7$
HEH[EHP]	$(1.56 \pm 0.08) \times 10^7$
TBP	$(1.17 \pm 0.26) \times 10^7$
DBBP	$(5.89 \pm 0.55) \times 10^7$
TBPO	$(1.50 \pm 0.14) \times 10^8$
TODGA	$(6.60 \pm 0.50) \times 10^8$
DEHBA	$(3.87 \pm 0.21) \times 10^8$
DEH*i*BA	$(7.98 \pm 0.80) \times 10^7$

The $NO_3^\bullet$ radical exhibited the fastest reactivity with the amidic ligands in dodecane, with rate constants ranging from $k = (7.98 \pm 0.80) \times 10^7$ for DEH*i*BA to $k = (6.60 \pm 0.50) \times 10^8$ M^{-1} s^{-1} for TODGA. By direct comparison of the structures of DEHBA and DEH*i*BA (see Figure 2) the factor of two increase in rate constant suggests that a dominant $NO_3^\bullet$ mechanism is through H-atom abstraction from the carbonyl-activated, adjacent, methylene (DEHBA) or amyl (DEH*i*BA) groups. This mechanism agrees with recent experimental measurements for the irradiation of pure DEHBA at 77K[35], where Electron Paramagnetic Resonance (EPR) measurements determined that three carbon-centered radicals were formed. From spectral fitting/simulation and Density Functional Theory (DFT) calculations using the PRIRODA—04 program developed by Laikov[36] at the (B3LYP)/L1a_3 level of theory[37,38] these radicals were identified as being immediately adjacent to the carbonyl group and N atom (total of ~89%) and in the aliphatic hexyl chains (~11%) within this molecule.

This proposed H-atom abstraction mechanism for $NO_3^\bullet$ radical reaction is also consistent with the measured 8x faster rate constant for TODGA, where H-atom abstraction from the central methylene groups activated by the two amide functional groups in this molecule would be expected. Again, this mechanism is supported by both 77K EPR experiments and corresponding DFT calculations,[35,39] where a similar mixture of three carbon-centered radicals is formed in this molecule (43% adjacent to the carbonyl group, 27% adjacent to the N atoms, and 30% in the outer aliphatic chains) under these frozen, pure-compound, conditions. Lastly, although the $NO_3^\bullet$radical reaction with TODGA reaction has not been investigated in other organic media, Mezyk *et al*. reported a similar value of (4.27 ± 0.46) x 10^8 $M^{-1}s^{-1}$ in *t*-butanol for the similar diamide *N,N*'-dimethyl-*N,N*'-dioctylhexylethoxymalonamide (DMDOHEMA),[19] again indicating similar reactivity in both non-polar solvents.

In contrast, the reactivity of $NO_3^\bullet$ with the phosphorus-based ligand TBP in dodecane was found to be the slowest measured here, with k_{12} = (1.17 ± 0.26) x 10^7 $M^{-1}s^{-1}$. This result is very similar to that of the measured rate constant of (1.42 ± 0.09) x 10^7 $M^{-1}s^{-1}$ previously reported by Mezyk *et al*. for nitrate radical reaction with TBP in *t*-butanol.[19] However, the rate constants for the organophosphorus compounds of this study *increased* in the order: phosphate (TBP,) < phosphonate (DBBP) < phosphine oxide (TBPO), inconsistent with only a H-atom abstraction mechanism occurring at the methylene groups immediately adjacent to the alkoxy O-atoms in these molecules. Recent DFT (Amsterdam Density Functional program[40], BP86, def2-TZVP basis sets) calculations for TBP, DBBP and TBPO showed that the Mulliken electronic charges on the phosphorus atoms in the P=O bond also increased in this order, with calculated values of +0.82, +0.73 and +0.58, respectively.[41] The oxygen atom in these bonds had a constant electronic charge of -0.51. This electron density on the basic phosphoryl oxygen not only gives phosphonates and

phosphine oxides their strong complexing ability for hard metal cations such as actinides and lanthanides. However, the increasing electron density at the phosphorus atom could also enhance the probability for a second electron abstraction mode of $NO_3^\bullet$ reaction,

$$TBPO + NO_3^\bullet \rightarrow [TBPO]^{\bullet+} + NO_3^- \quad (16)$$

giving these ligands overall faster $NO_3^\bullet$ reaction rate constants. While rate constants approaching the diffusion-controlled limit (ca. 10^{10} M^{-1} s^{-1} [14]) have been attributed to electron transfer reactions[42] our slower values are consistent with the abstraction occurring from these relatively electron density positive phosphorus atoms.

We previously reported that alcohols and alkanes have slower rate constants for the $NO_3^\bullet$ radical reaction than do aromatic compounds, indicative of H-atom abstraction reactions occurring for the alkanes.[19] This finding is also consistent with the conclusions of He *et al*., who previously reported that $NO_3^\bullet$ reacted by H-atom abstraction from the alkyl chains of TBP, citing as evidence the increasing rate constants for reaction with analogs of increasing alkyl chain length.[30] However, our proposed additional mechanism for electron abstraction from the phosphorus atom is supported by previous kinetic measurements for aqueous hydroxyl ($^\bullet$OH) radical reactions with a series of chemical warfare agent simulants where based on a Bronsted analysis of the kinetics and the pKa values for the non-ethoxy groups in these phosphonates the initial reaction was attributed to direct oxidation occurring at the phosphorus atom.[43,44]

A phosphoric acid ligand, HEH[EHP] (see Figure 1), was also investigated in this study. Acidic extractants such as HEH[EHP] have found utility for the complexation of actinides and lanthanides in aqueous solutions of low acidity, such as are used for separating lanthanides into the organic phase while the actinides are retained in the aqueous phase by a soft-donor complexing agent.[45] The HEH[EHP] was found to have a slow rate constant of (1.56 $\pm$ 0.08) x 10^7 $M^{-1}s^{-1}$,

reflecting both the lower electron density on its phosphoryl oxygen and the steric hindrance to H-atom abstraction introduced by its branched alkane chains. In addition, at the ligand concentrations of 0.2–30 mM used in these kinetic studies HEH[EHP] has been shown to dimerize to reduce the repulsion of the polar phosphate group in the non-polar medium, which would further hinder reaction of $NO_3^{\bullet}$ radical with the central methylene groups or P atoms. Kimberlin and Nash reported the dimer association constant in *n*-dodecane to be K = 5500,[46] which for our HEH[EHP] concentration range would correspond to a dimer fraction ranging from 25 to 47%. However, as no calculated electron charges for the $(HEHEHP)_2$ dimer could be found in the literature we were unable to quantify the Mulliken value trend for the HEHEHP phosphorus atom in this group of ligands.

Regardless of mechanistic considerations, all ligands investigated showed relatively slow rate constants relative to the diffusion-limited rate but certainly still high enough to have consequences under solvent extraction conditions. The reaction of $NO_3^{\bullet}$ with dodecane was reported to have a slow bimolecular-rate constant of $(6.45 \pm 0.33) \times 10^6$ $M^{-1}s^{-1}$ in *t*-butanol,[19] and presumably has a similar slow rate constant in concentrated (4.4 M) dodecane solution. Therefore, even millimolar ligand concentrations are expected to compete for produced $NO_3^{\bullet}$ in dodecane solution. For example, given a typical process concentration of 200 mM TODGA in dodecane,[47] a relative rates analysis indicates that the TODGA will scavenge up to 80% of produced $NO_3^{\bullet}$, resulting in decreasing ligand concentrations and the production of ligand oxidation products. Continued investigations of these kinetics are warranted to acquire the data necessary to model the radiation chemistry of dodecane solutions.

Conclusions:

These first-ever reported bimolecular rate constants for the reaction of the $NO_3^{\bullet}$ radical in dodecane solution indicate rates fast enough to result in significant oxidation for the ligand concentrations used in nuclear solvent extraction applications. For neutral organophosphorous ligands, the rates increased with increasing O-donor basicity, reflecting an increasing contribution of electron transfer over H-atom abstraction reactions. For the acidic organophosphorous ligand measured the rates were slow, probably mostly because of its known dimerization at the investigated concentrations. The amidic ligands had overall higher reaction rates, again reflecting an increased contribution for electron transfer reactions. Oxidation of ligands by $NO_3^{\bullet}$ radical will result in decreases in ligand concentration and nitration of ligand molecules, with attendant effects of separation efficiency for actinide and lanthanide ions. The rate constants measured here in dodecane will be among important data needed to model the radiolysis reactions in the organic phase for nuclear solvent extraction.

Conflicts of interest

There are no conflicts to declare.

Acknowledgments

This research was performed using funding received from the U.S. Department of Energy (DOE) Nuclear Energy University Program (NEUP), award DE-NE0008659. The laser photolysis work reported herein was conducted at the Radiation Research Laboratory, University of Notre Dame, supported by the Division of Chemical Sciences, Geosciences and Biosciences, Basic Energy sciences, Office of Science, United States Department of Energy, under Award DE-SC0021372. Work performed at Idaho National Laboratory was under DOE operations contract no. De-AC07-05ID14517.

Notes and references

1 E.R. Irish and W.H. Reas, *The PUREX process: A Solvent Extraction Reprocessing Method for Irradiated Uranium*, Hanford Atomic Products Operation, Hanford WA, 1957.
2 W.W. Schulz and J.D. Navratil, *Science and Technology of Tributyl Phosphate*, CRC Press, Boca Raton, FL, USA 1984
3 R.R. Shoun and W.J. McDowell, Actinide Extractants: Development, Comparison and Future, Ch. 6 in: *Actinide Separations, ACS Symposium Series 17*, American Chemical Society, Washington D.C., USA, 1980.
4 D. Xu, Z. Shah, Y. Cui, L. Jin, X. Peng, H. Zhang and G. Sun, *Hydrometallurgy*, 2018, **180**, 132.
5 Y. Sasaki, Y. Sugo, K. Morita and K. L. Nash, *Solvent Extr. Ion Exch*., 2015, **33**, 625.
6 S. Tachimori and Y. Morita, Overview of Solvent Extraction Chemistry for Reprocessing, Ch. 1 in: *Ion Exchange and Solvent Extraction, A Series of Advances*, CRC Press, Boca Raton, FL, USA, 2010.
7 G. Elias, B.J. Mincher, S.P. Mezyk, T.D. Cullen and L.R. Martin, *L.R. Environ. Chem*. 2010, **7**, 183.
8 S.P. Mezyk, T.D. Cullen, T.D. G. Elias and B.J. Mincher, Aqueous Nitric Acid Radiation Effects on Solvent Extraction Process Chemistry, Ch. 16, in *Nuclear Energy and the Environment, ACS Symposium Series 1046*, American Chemical Society, Washington D.C., USA, 2010.
9 M. Daniels, *J. Phys. Chem.* 1966, **70**, 3022.
10 M. Daniels, *J. Phys. Chem*. 1969, **73**, 3710.
11 Y. Katsumura, P. Y. Jiang, R. Nagaishi, T. Oishi, and K. Ishigura, *J. Phys. Chem*. 1991, **95**, 4435.
12 Y. Katsumura, $NO_2^{\bullet}$ and $NO_3^{\bullet}$ radicals in radiolysis of nitric acid solutions, in: *N-centered Radicals*, Wiley and Sons, NY, 1998.
13 E. Kozlowska-Milner and R.K. Broszkiewicz, *Radiat. Phys Chem*. 1978, **11**, 253.

14 G.V. Buxton, C.L. Greenstock, W.P. Helman, and A.B. Ross. *J. Phys. Chem. Ref. Data*, 1988, **17**, 513.
15 J. Ma, F. Wang and M. Mostafavi, *Molecules*, 2018, **23**, 244.
16 M.M. Maguta, Y. Stenstrøm, Y. and C.J. Nielsen, *J. Phys. Chem. A* 2016, **120**, 6970.
17 N.L. Ng, S.S. Brown, A.T. Archibald, E. Atlas, R.C. Cohen, J.N. Crowley, D.A. Day, N.M. Donahue, J.L. Fry, H. Fuchs, R.J. Griffin, M.I. Guzman, H. Herrmann, A. Hodzic, Y. Iinuma, J.L. Jimenez, A. Kiendler-Scharr, B.H. Lee, D.J. Luecken, J.Mao, R. McLaren, A. Mutzel, H.D. Osthoff, B. Picquet-Varrault, U. Platt, H.O.T. Pye, Y. Rudich, R.H. Schwantes, M. Shiraiwa, J. Stutz, J.A. Thornton, A. Tilgner, B.J. Williams, and R.A. Zaveri, *Atmospheric Chem. Phys.* 2017, **17**, 2103–2162.
18 C.A. Cantrell, NO*x* in the atmosphere, in: *N-centered Radicals*, Wiley and Sons, NY, 1998.
19 S.P. Mezyk, T.D. Cullen, K. A. Rickman and B.J. Mincher, B. J. *Int. J. Chem. Kinet.* 2017, **49**, 635.
20 G.P. Horne, W. Wilden, S.P. Mezyk, M. Hupert, A. Stärk, W. Verboom, B.J. Mincher and G. Modolo, *Dalt. Trans*. 2019, **48**, 17005.
21 B.J. Mincher and R.D. Curry, *App. Rad. Isot*. 2000, **52**, 189.
22 J.R. Ferraro, M. Borkowski, R. Chiarizia, and D.R. McAlister, D.R. *Solv. Extr. Ion Exch*. 2001, **19**, 981.
23 G.P. Horne, C.A. Zarzana, T.S. Grimes, C. Rae, J. Ceder, S.P. Mezyk, B.J. Mincher, M.-C. Charbonnel, P. Guilbaud, G. Saint-Louis, and L. Berthon, L. *Dalt. Trans*. 2019, **48**, 14450.
24 G.S. Groenewold, G. Elias, B.J. Mincher, S.P. Mezyk, and JA. LaVerne, *Talanta*, 2012, **99**, 909.
25 G. Elias G.S. Groenewold, B.J. Mincher and S.P. Mezyk, *J. Chromatography A*, 2012, **1243,** 47.
26 D. Woodhead, F. McLachlan, R. Taylor, U. Mullich, A. Geist, A. Wilden, and G. Modolo, *Solv. Ext. Ion Exch*., 2019, **37**, 173.
27 G. Hall, T. Levitskaia and K.L. Nash, *Solv. Ext. Ion Exch*. 2018, **36**, 331.
28 K. Bell, A. Geist, F. McLachlan, G. Modolo, R. Taylor and A. Wilden, A. *Procedia Chem*. 2012, 7, 152.
29 Z.B. Alfassi, S. Padmaja, P. Neta, R.E. Huie, *J. Phys. Chem* 1993, **97**, 3780.
30 H. He, M. Lin, Y. Muroya, H. Kudo and Y. Katsumura. *Phys. Chem. Chem. Phys.* 2004, **6**, 1264–1268.
31 G.L. Hug, *Optical Spectra of nonmetallic inorganic transient species in aqueous solution*, NSRDS-NBS 69, US Department of Commerce, National Bureau of Standards, 1981.
32 R.W. Glass and T.W. Martin, *J. Am. Chem. Soc.* 1970, **92**, 5084
33 L.K. Wan, J. Peng, M. Z. Lin, Y. Muroya, Y. Katsumura and H. Y. Fu, *Radiat. Phys. Chem.,* 2012, **81**, 524.
34 C.A. Buchanan, D. Herrera, M. Balasubramanian, B.R. Goldsmith and N. Singh, *JACS Au*, 2022, **2**, 12742.
35 I.S. Sosulin and A.Lisouskaya, *Rad. Phys. Chem.* 2024, **222**, 111785.
36 D.N. Laikov, and Y.A. Ustynyuk, *Russ. Chem. Bull.* 2005, **54**, 820.
37 D.N. Laikov, *Chem. Phys. Lett*. 2005, **416**, 116.
38 D.N. Laikov, Theor. Chem. Acc., 2019, **138**, 40.

39. I.A. Shkrob, T.W. Marin, J.R. Bel, H. Luo, S. Dal, J.L. Hatcher, R.D. Rimmer, J.F. Wishart, *J. Phys. Chem. B.,* 2012, 116, 2234.
40. SCM, ADF 2016; Theoretical Chemistry, V. U. A., The Netherlands. 2016 http://www.scm.com/
41. A.R. Sachin, G. Gopakumar, C.V.S.B. Rao, S. Nagarajan, *Comp. Chem.*, 2024, **45**, 70.
42. P. Neta and R.E. Huie *J Phys Chem* 1986, **90**, 4644.
43. J.J. Kiddle and S.P. Mezyk, *J. Phys. Chem. B*, 2004, **108**, 9568.
44. A. Abbott, T. Sierakowski, J.J. Kiddle, K.K. Clark, S.P. Mezyk, *J. Phys. Chem. B*, 2010, **114**, 7681.
45. J.C. Braley, T.S. Grimes, and K.L. Nash, *Ind. Eng. Chem. Res*. 2012, **51**, 629.
46. A. Kimberlin and K.L. Nash, *Solv. Ext. Ion Exch*., 2021, **39**, 38.
47. D. Peterman, A. Geist, B. Mincher, G. Modolo, M.H. Galán, L. Olson, and R. McDowell, *Ind. Eng. Chem. Res*., 2016, **55**, 10427.

CALIFORNIA STATE UNIVERSITY, LONG BEACH
DEPARTMENT OF CHEMISTRY AND BIOCHEMISTRY

July 01, 2024

To Whom it May Concern:

The data that support the findings of this study are available on request from the corresponding author.

Sincerely,

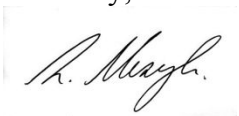

Stephen Mezyk Ph.D.